Transactions of ASME, Journal of Dynamics, Measurement and Control, Vol. 109, No. 2, pp. 73-79.

MOTION CONTROL ANALYSIS OF A MOBILE ROBOT

by
Johann Borenstein[+] and Yoram Koren[++]

ABSTRACT

A computer-controlled vehicle that is part of a mobile nursing robot system is described. The vehicle applies a motion control strategy that attempts to avoid slippage and minimize position errors. A cross-coupling control algorithm that guarantees a zero steady-state orientation error (assuming no slippage) is proposed and a stability analysis of the control system is presented. Results of experiments performed on a prototype vehicle verify the theoretical analysis.

[+] Graduate Student
[++] Professor, Member ASME
Faculty of Mechanical Engineering
Technion, Israel Institute of Technology
Haifa, Israel
Submitted to the ASME in May 1985; revised May 1986 and November 1986

Nomenclature

b	= Distance between the drive wheels
c	= Proportionality constant [rad/pulse]
D_j	= Torque disturbance in loop j, [Nm]
ΔD	= Difference between torque disturbances
d	= Nominal diameter of the drive wheels
E	= Position difference between both motors [pulses]
E'	= Orientation error [radians]
F_j	= Encoder frequency in loop j [pulses/s]
H	= Encoder gain
K	= Open-loop gain
K_a	= Digital-to-analog converter (DAC) gain
K_b	= Motor constant including the gain of the power amplifier
K_c	= Integral gain
K_p	= Proportional gain
L	= Distance traveled M = Correction variable
P_j	= Position of the motor in loop j [pulses]
R_j	= Required velocity in loop j
r	= Repeatability distance [cm]
T	= Sampling time
U_j	= Velocity error in loop j
u	= Difference in diameter of both wheels
x_0	= Initial X-coordinate
x_f	= Final X-coordinate
y_0	= Initial Y-coordinate
y_f	= Final Y-coordinate
Δx	= Translatory motion per encoder pulse
α	= Disturbance factor
β	= Direction flag
θ_0	= Initial orientation
θ_f	= Final orientation
$\theta_{1/2}$	= First/second rotation
$\Delta\theta$	= Orientation error [rad]
ρ	= Radius of the curved path due to different wheel diameters
τ	= Loaded motor time constant
ϕ	= Slope of straight line connecting initial and final positions
ω_j	= Angular velocity in loop j [rev/s]

1. Introduction

This paper discusses the control of an autonomous vehicle that is part of a nursing robot system, developed at the Technion. The nursing robot is intended to be an aid for the bedridden, who require constant assistance for the most elementary needs such as fetching a glass of water, operating electrical appliances, or replacing a cassette in a video recorder.

A prototype of the nursing robot is shown in Fig. 1. It comprises two main components: A vehicle that houses the computers and electronic hardware, and a commercially available five degree-of-freedom manipulator. The vehicle moves to a target location and subsequently the manipulator performs its task (e.g., fetching a book). Then the vehicle moves again to complete the instruction.

Most of the design considerations of the nursing robot are also applicable to household robots, which may be practicable by the end of this decade [1]. Mobile robots are also candidates for mining and farming applications, as well as for transportation in nuclear plants [2] and factories [3]. Therefore, the nursing robot will be discussed throughout this paper as a general mobile robot.

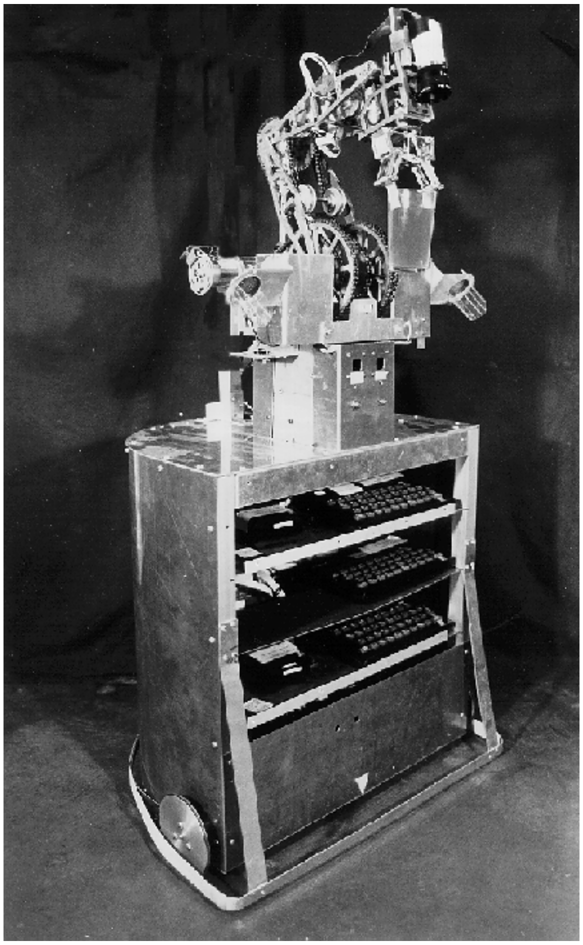

Fig.1: The Technion's Nursing Robot.

2. Design Considerations for Mobile Robots

A design frequently used for computer-controlled vehicles consists of two drive wheels, each with its own controlled DC motor or stepping motor [4-10]. One or two free-wheeling castors provide stability. Such a design was chosen for the vehicle of the nursing robot, as shown in Fig. 2. Two DC motors, with built-in reduction gears and incremental encoders, drive two wheels constituting the front axle of the vehicle. The resolution of the encoders is such that one pulse represents 2 mm of tangential travel of the drive wheel. The motors are coupled to the wheel shafts through a 65.5:1 gear ratio. In the rear, there is one free-wheeling castor. Although castors have been said to cause slipping during direction changes [11], it has been proven that this is may not always occur [12].

A more complicated design that allows three DOF-motion in the plane and is based on three wheel-pair assemblies was presented in [13,14]. However, this vehicle has been found to be very difficult to control [15] and no satisfactory solution has been found yet [16].

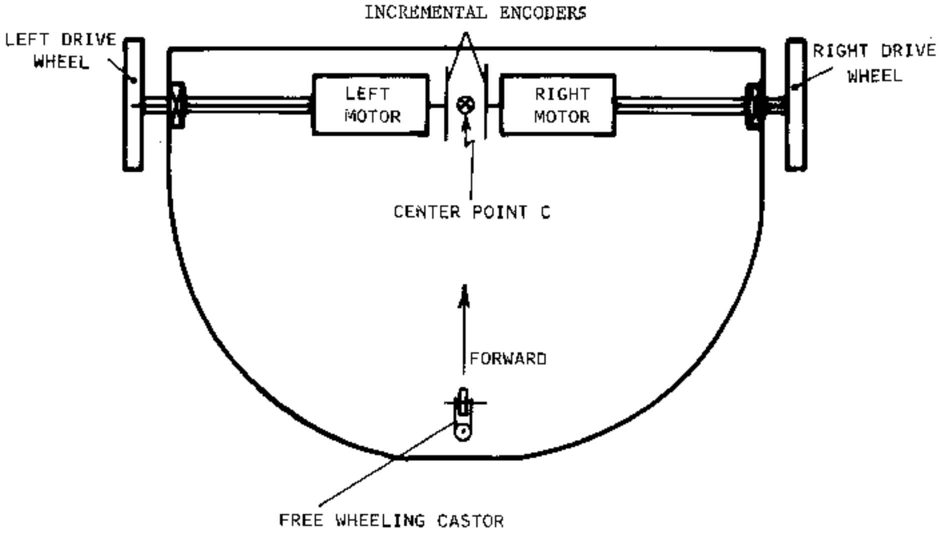

Figure 2: Diagram of the mobile platform.

In mobile robots it is desirable to place the two drive wheels as far apart as possible, for the following reasons:

1. The stability of the vehicle is improved.

2. The effect of the encoder resolution on the orientation error of the vehicle is decreased. In the worst case, the orientation error $\Delta\theta$ is given approximately by

$$\Delta\theta = \frac{\Delta x}{b} \tag{1}$$

   As seen from Eq. (1), the orientation error $\Delta\theta$ is reduced by increasing the distance between the drive wheels (b).

3. During straight-line motion, mechanical disturbances might cause the motors to run temporarily at different angular speeds, resulting in a temporarily curved path. It can be shown by trigonometry that the radius of the curved path is directly proportional to the wheel separation distance b.

4. Differences in the two wheel diameters will also cause a curved path with a radius proportional to the distance b.

On the other hand, an exaggerated base width will adversely affect the mobility within a room. In the present design the distance between the two drive wheels is 600 mm.

The position and the orientation of the mobile nursing robot in a room is determined by two alternate sensing methods; incremental and absolute. When the vehicle is in motion, its position is measured by the incremental encoders attached to the wheels. The incremental position is accumulated by the control computer, which in t urn determines the position and the orientation of the robot in the room. When the vehicle is at rest, an absolute position measuring system is employed to compensate for the inaccuracies of the incremental method. It comprises three light sources attached to the room's walls and a rotating light-detecting sensor located on the first joint of the robot. This approach periodically updates the absolute position and orientation of the vehicle, and therefor requires the vehicle's position accuracy while traveling to be relatively high (e.g., a deviation of 1 cm for 1 m traveling distance). Therefore, the avoidance of wheel slippage is extremely important.

Wheel slippage occurs mainly during two types of motions: (a) acceleration and deceleration, and (b) during non-straight-line motions where centrifugal forces cause lateral slippage. The latter effect is minimized by limiting non-straight-line motions to "on-the-spot" rotation, where both drive wheels run at the same speed but in opposed directions. In this case, and with symmetric weight distribution, no lateral forces occur at the wheels. Slippage during the acceleration and deceleration phases is reduced by employing low acceleration and deceleration rates (the maximum speed is 0.27 m/s).

Another approach to minimize the effect of slippage is to mount the encoders on two additional freely rotating wheels driven by the vehicle's motion. By dividing the tasks of driving the vehicle and providing feedback information between two sets of wheels, each wheel set may be appropriately designed for its task. The additional wheels were not included in our vehicle, since the experimental results obtained with the encoders mounted directly on the drive wheels are satisfactory for the nursing robot purposes. However, for applications in which more accurate positioning of the vehicle is required, the two feedback wheels should be added.

3. Motion Control

Motion control means the strategy by which the vehicle approaches a desired location and the implementation of this strategy.

Motion Types

The nursing robot vehicle is designed to perform only two distinct kinds of motion: straight-line motion, where both motors are running at the same speed and in the same direction, and rotation about the vehicle's center-point, where both motors are running at the same speed but in opposite directions. This approach is advantageous for several reasons:

1. Wheel slippage is minimized because of the simultaneous action or rest of both wheels and because of the "on-the-spot" rotation action for turns.

2. A relatively simple control system may be used, since in either case the only task of the controller is to maintain equal angular velocities,

3. The vehicle path is always predictable, unlike other motion strategies which smooth sharp corners by an unpredictably curved path (e.g., [17]). A predictable path is advantageous when global path planning, to avoid obstacles, is employed.

4. The vehicle always travels through the shortest possible distance (straight-line or "on-the-spot" rotation).

The Control Algorithm

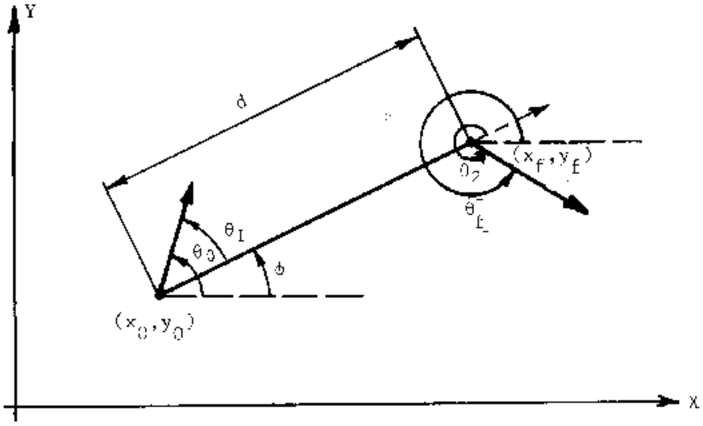

Fig.3: Procedure for traveling to a new location.

In order to represent the vehicle location relative to a fixed coordinate system, three values must be given: the X and Y coordinates of the centerpoint, C, and the angle θ_0 between the vehicle's longitudinal axis and the X-axis.

If the vehicle has to travel from a known present location (x_0, y_0, θ_0) to a new location (x_f, y_f, θ_f), as illustrated in Fig. 3, the following procedure is performed to determine a trajectory. First, the distance L and the slope ϕ of the straight line connecting the present and final locations are calculated:

$$\phi = \arctan\frac{y_f - y_0}{x_f - x_0} \tag{2}$$

$$L = \sqrt{(x_f - x_0)^2 + (y_f - y_0)^2} \tag{3}$$

The vehicle then turns θ_1 degrees about its centerpoint, which is calculated by $\theta_1 = \phi - \theta_0$. Next, it travels along a straight line of the distance L so that its centerpoint will be at (x_f, y_f). Finally, the vehicle turns θ_2 degrees about its centerpoint, where $\theta_2 = \theta_f - \phi$.

For each of these steps the number of pulses that each motor must produce in order to complete the command is calculated. This number is always equal for both motors. However, during vehicle rotation both motors rotate in opposite directions, and during straight-line motion they rotate in the same direction. The calculations of L, ϕ, θ_1 and θ_2 are performed before the vehicle begins to move, and therefore they do not affect the sampling rate of the control loop.

4. Control System Analysis

A conventional controller for a mobile robot consists of two independent control loops, one for each motor. A similar approach is sometimes used to drive the worktable of CNC milling machines or Cartesian robots [18,19]. Motion coordination in these systems is achieved by adjusting the reference velocities of the control loops, but the loop of one axis receives no information regarding the other. Any load disturbance in one of the axes causes an error that is corrected only by its own loop, while the other loop carries on as before. This lack of coordination causes an error in the resultant path. An improvement in the path accuracy can be achieved by providing cross-coupling, whereby an error in either axis affects the control loops of both axes. A cross-coupling method was applied to a Japanese mobile robot [20], in which each loop used the position error of the other loop, but a signal proportional to the resultant path error was not generated. A control analysis is not provided in [20] and experimental results are not reported.

The controller used here, applies an approach similar to the cross-coupled controller, which has been found to be advantageous for two-axis NC and CNC systems [21]. In this design the path error is calculated and fed as a correction signal to both loops. The main differences between the present design and the one used in CNC systems are that here the absolute reference velocities to both axes are always equal and the controller always maintains the maximum allowable speed of the motors, thus enabling the use of smaller motors since they are utilized at their maximum performance level.

The vehicle controller consists of a dedicated microcomputer and the peripheral hardware that is seen in Fig. 4. It is designed to issue an 8-bit binary speed command for each motor. The command is converted by a digital-to-analog converter (DAC) into an analog signal, amplified, and used to drive the motor. The encoder produces two 90^{o} phase-shifted pulse trains that are fed into a directional sensing circuit (DSC), which issues an appropriate pulse train to a 4-bit up-down counter. The counter also serves as a buffer, since the encoder pulses are transmitted faster than can be sampled. An inhibit signal is provided by the DSC in order to avoid the counter reading at the instant when its state is changed. At each iteration (40 ms), the contents of both counters are simultaneously sampled and added to associated software counters. Subsequently, the hardware counter is reset. Thus, each software counter holds a number that represents the total number of pulses generated since the beginning of a certain motion. A comparison between the absolute values of both software counters produces the error signal E

$$E(I) = |\, P_1(I) \,| \; - \; |\, P_2(I) \,| \tag{4}$$

A non-zero E indicates that one motor has been running faster than the other, and the sign of E identifies that motor. The error signal generates a correction variable M that is used to reduce the speed of the faster motor, and thereby the velocities of both motors are equalized. Absolute values of P_1 and $P_2$are used in Eq. (4) in order to account for rotational motion, in which both motors run in opposite directions.

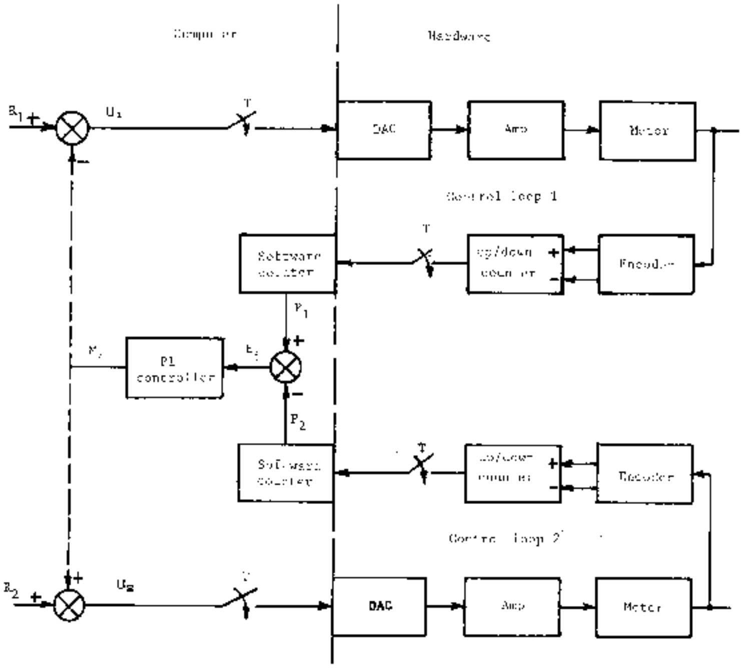

Figure. 4: The control loops of the mobile platform.

Any temporary disturbance of the steady-state velocities will be successfully corrected by a proportional (P) controller. However, in order to correct a continuous disturbance, as might be caused by different friction forces in the bearings (e.g., due to an asymmetric load distribution on the vehicle), an integral (I) action is required as well. The PI-controller provides not only equal velocities but also an equal overall pulse count from the beginning of each motion. Therefore, this controller guarantees a zero steady-state orientation error of the vehicle for any constant continuous disturbance (except for slippage).

The equations of the PI-controller are

$$S(I) = S(I\text{-}1) + E(I) \tag{5}$$

$$M(I) = K_c S(I) + K_p E(I) \tag{6}$$

where K_c is the integration gain and K_p is the proportional gain. The ranges of K_c and K_p that guarantee stability of the system have been determined as described in the following table:

H	= 3 pulses/rev
K_a	= 0.02 volt/pulse
K_b	= 18.4 rev/volt
K_c	= 1 $\sec^{-1}$
K_p	= 12
T	= 0.04 sec
α	= 1.0 volt/Nm
τ	= 0.2 sec

The block diagram of the entire control loop is shown in Fig. 5. The motor is approximated as first-order lag which in Laplace notation (including the encoder) is

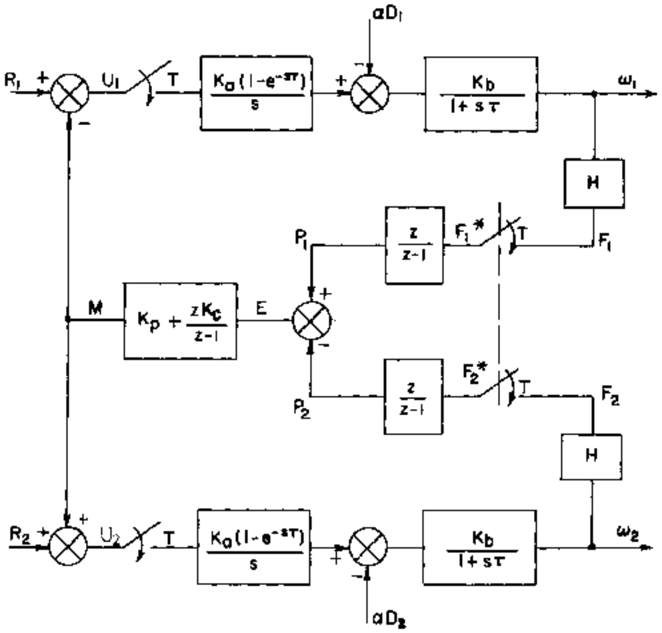

Figure. 5: Block diagram of the control system.

$$F_j(s) = \frac{HK_b}{1+s\tau}(V_j - \alpha D_j) \qquad j = 1, 2 \tag{7}$$

In the DAC the signal is held constant during the interval *T*, and therefore its transfer function is that of a zero-order hold (ZOH):

$$\frac{V_j}{U_j}(s) = \frac{K_a(1 - e^{-sT})}{s} \tag{8}$$

Substituting Eq. (8) into (7) yields

$$F_j(s) = \frac{HK_aK_bU_j(1 - e^{-sT})}{s(1 + s\tau)} - \frac{HK_b\alpha D_j}{(1 + s\tau)} \tag{9}$$

Performing the Z-transform on Eq. (9) yields

$$F_j(z) = K\frac{(1-r)}{(z-r)}U_j(z) - HK_b\frac{z\omega}{(z-r)}\alpha D_j(z) \tag{10}$$

where K is the open-loop gain given by $K = K_a K_b\, H = 0.02 \cdot 18.4 \cdot 3 = 1.1$ pulses/(s · volt) and r and ω are defines as

$$r = \exp(-\frac{T}{\tau}) = \exp(-\frac{0.04}{0.2}) = 0.82$$

$$\omega = \frac{1}{\tau} = 5s^{-1}$$

The software control algorithm may be represented with the aid of the Z-transform as

$$P_j(z) = \frac{z}{z-1}F_j(z) \qquad j = 1, 2 \tag{11}$$

$$E(z) = P_1(z) - P_2(z) = \frac{z}{z-1}(F_1(z) - F_2(z)) \tag{12}$$

$$M(z) = (K_p + K_c\frac{z}{z-1})E(z) \tag{13}$$

$$U_1(z) = R_1(z) + \beta_1 M(z) \tag{14a}$$

$$U_2(z) = R_2(z) + \beta_2 M(z) \tag{14b}$$

where $\beta_1 = 0$ and $\beta_2 = 1$, for negative M
and $\beta_1 = 1$ and $\beta_2 = 0$, for positive M

Substituting Eqs. (13) and (14) into Eq. (10) gives

$$F_1(z) = K(\frac{1-r}{z-r})\,[R_1(z) + \beta(K_p + K_c\frac{z}{z-1})E(z)] - HK_b(\frac{z\omega}{z-r})\alpha D_1(z) \tag{15a}$$

$$F_2(z) \; = \; K(\frac{1-r}{z-r})\,[R_2(z)+\beta(K_p+K_c\frac{z}{z-1})E(z)] \; - \; HK_b(\frac{z\omega}{z-r})\alpha D_2(z) \qquad (15b)$$

For straight-line motion $R_1 = R_2$ and therefore the difference between these two signals is

$$F_1(z)-F_2(z) \; = \; -K(\frac{1-r}{z-r})(K_p+K_c\frac{z}{z-1})E(z) \; + \; HK_b(\frac{z\omega}{z-r})\Delta D(z) \qquad (16)$$

where

$\Delta D(z) = \alpha D_2(z) - \alpha D_1(z)$

Substituting Eq. (16) into Eq. (12) gives the solution of $E(z)$

$$E(z) \; = \; \frac{z}{z-1}[-K(\frac{1-r}{z-r})(K_p+K_c\frac{z}{z-1})E(z) \; + \; HK_b(\frac{z\omega}{z-r})\Delta D(z)] \qquad (17)$$

The corresponding transfer function is

$$\frac{E(z)}{\Delta D(z)} \; = \; \frac{z^2(z-1)HK_b\omega}{(z-1)^2(z-r)+z(z-1)KK_p(1-r)+z^2KK_c(1-r)} \qquad (18)$$

with the characteristic equation

$$Q(z) \; = \; z^3+[K(1-r)(K_p+K_c)-(2+r)]z^2 \; + \; [1+2r-K(1-r)K_p]z \; - \; r \qquad (19)$$

We define

$$Q(z) \; = \; a_3z^3+a_2z^2 \; + \; a_1z \; - \; a_0 \qquad (20)$$

where

$a_3 = 1$
$a_2 = K(1\text{-}r)(K_p + K_c) - (2+r)$
$a_1 = 1 + 2r - K\,K_p\,(1\text{-}r)$
$a_0 = -r$

Jury's stability criterion [22] requires that the following four conditions are satisfied:

1. $Q(z=1) > 0$ (21)

This condition yields

$$K_c > 0 \tag{22}$$

2. $Q(z=-1) < 0$ (23)

which gives

$$K_c < \frac{4(1+r)}{K(1-r)} = 2K_p \tag{24a}$$

or, by substituting the values for K and r

$$K_c < 36 - 2K_p \tag{24b}$$

3. $| a_0 | < a_3$ (25)

This condition is always satisfied and adds no information.

4. $| b_0 | > b_2$ (26)

where

$$b_0 = \begin{bmatrix} a_0 & a_3 \\ a_3 & a_0 \end{bmatrix} \qquad b_2 = \begin{bmatrix} a_0 & a_1 \\ a_3 & a_2 \end{bmatrix}$$

namely

$$1\text{-}r^2 > | -(1\text{-}r^2) + K(1\text{-}r)^2K_p - K(1\text{-}r)rK_c | \tag{27}$$

Equation (27) contains two cases:

a. $b_2 < 1 - r^2$

which yields

$$K_c > K_p(\frac{1}{r} - 1) - \frac{2(1-r^2)}{K(1-r)r} \tag{28a}$$

and after substitution of K and r

$$K_c > 0.22K_p - 4 \tag{28b}$$

b. $b_2 > -(1-r^2)$

which yields

$$K_c < K_p(\frac{1}{r} - 1) \tag{29a}$$

and by substituting r

$$K_c < 0.22K_p \tag{29b}$$

The three inequalities (22), (24), and (29) define a range in the K_c - K_p plane in which stability is guaranteed. in order to verify the analysis, the prototype vehicle was tested with several gain values. The results (stable = '+', unstable = '-') have been plotted in Fig. 6, and most of them fit the theoretical analysis. Figure 7 shows typical experimental results of the error E as a response to a step input in the Disturbance D for K_p = 12 and three K_c gain values. For K_c = 3 the system is unstable. it is undesirable to select gains that are too close to the boundaries in Fig. 6 (e.g., the left zone in which $K_p < 9$ or the upper zone in which $K_c > 2$). We selected the values K_p = 12 and K_c = 1 for the nursing robot vehicle.

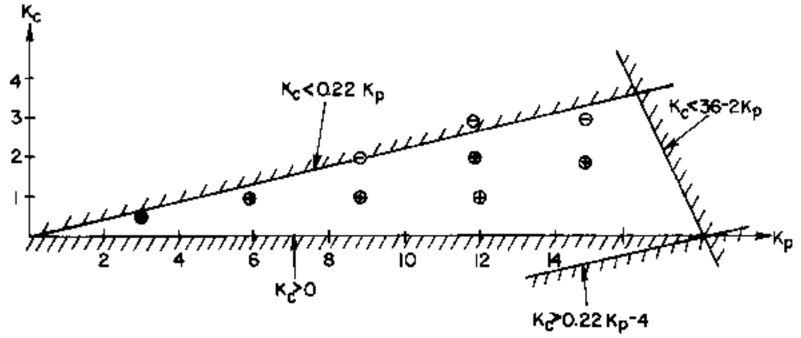

Figure. 6: Allowable range for the gains K_p and K_c, with experimental results. (+ = stable, - = unstable)

in order to show that the steady state orientation error E'_{ss} due to a continuous disturbance ΔD_0 is zero, one must recall that the orientation error E' is directly proportional to the difference between the accumulated pulse counts of both motors, such that

$$E' = c(P_1 - P_2) = cE \tag{30}$$

Substituting the difference in disturbing torques

$$\Delta D(z) = \frac{z}{z-1}\Delta D_0 \tag{31}$$

and Eq. (18) into Eq. (31) yields

$$E'(z) = c\frac{z^2(z-1)HK_b\omega\frac{z}{z-1}\Delta D_0}{(z-1)^2(z-r)+z(z-1)KK_p(1-r)+z^2KK_c(1-r)} \tag{32}$$

Applying the final value theorem shows that the steady-state orientation error is zero:

$$E'_{ss} = \lim_{z\to 1}(z-1)E'(z) = 0 \tag{33}$$

as was claimed above.

5. Experimental Results

The vehicle shown in Fig. 1 was tested. Experiments have shown that the position errors recorded by the control system are very small, on the order of magnitude of 10 mm per 10 m straight travel [12].

In one test the vehicle was programmed to travel along a figure-eight path with an overall length of about 13 m. The path, as recorded by the control system, is shown in Fig. 8a. After returning to the original starting location, the vehicle's calculated path position error (*E*) was less than 10 mm lateral and less than 1° rotational. This error does not include mechanically induced accuracies. The *real* position error, including mechanical inaccuracies and *actually* measured on the floor (external to the robot), was 6 cm lateral and 1° rotational. These results compare favorably to the results of a similar experiment described in [17]. A plot of one of the results in [17] has been reproduced here (Fig. 8b) for comparison. However, the vehicle used in [17] was faster, heavier, and did not halt at the corners of the programmed path.

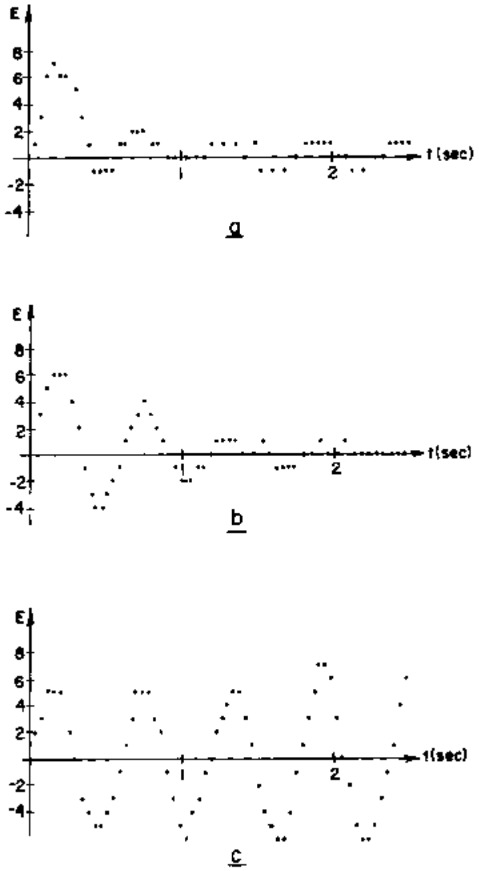

Figure. 7: Experimental response to a step disturbance with K_p=12 and
a) K_c = 1 b) K_c = 2 c) K_c = 3

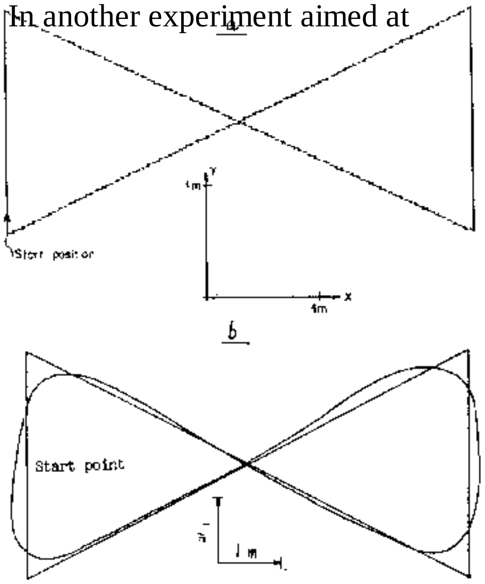

Figure. 8: Actual trajectory for the figure eight shape path.
a) The Nursing Robot
b) Robot in [17].

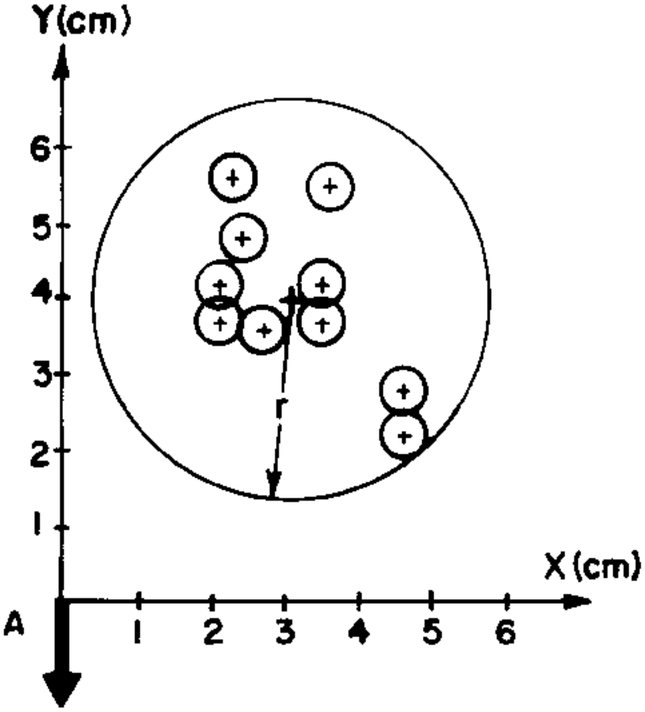

Figure. 9: Repeatability for a 2 m by 2 m square shape path.

In another experiment aimed at determining the vehicle's repeatability, the vehicle was programmed to follow a 2 × 2 m square path, such that its final location (position and orientation) should be identical to the initial one. Ten tests were performed and in each of them the vehicle's actual position upon completing the square path was plotted on the floor, as indicated by the small circles in Fig. 9. For this experiment, the mean error was 5.11 cm and the repeatability was r = 2.7 cm, where *r* is defined as the radius of the smallest circle surrounding all end points [23].

6. Conclusions and Discussion

A cross-coupling control scheme for mobile robots was presented. The controller guarantees a zero steady-state orientation error despite continuous torque disturbances. An analysis that provides boundary conditions for stability was presented. Experimental verification on a prototype mobile robot was demonstrated, and the resultant position errors are significantly small.

The position accuracy of our mobile robot is mainly affected by mechanical disturbances, the most severe of which are discussed below.

1. In order to minimize slip, the contact surface between wheels and floor should have a high friction coefficient, so rubber wheels are used. However, it is difficult to obtain rubber wheels with exactly the same diameter. In addition, unequally distributed loads will slightly

compress one wheel more than the other, thus changing its rolling radius. Wheels with different diameters cause the vehicle to travel along an arc, rather than along a straight line, even if the motors are running at equal speeds. A rigid wheel design [7] is therefore preferable. In our vehicle, accurately milled wheels with a 2-mm coating ("tire") were utilized.

2. There is a contact area, rather than a contact point, between the wheel and the floor. This causes an uncertainty about the effective distance between the drive wheels, creating inaccuracies when turning.

3. Another major mechanical disturbance is caused by the misalignment of the drive wheels. This effect will produce a lateral drag force resulting in a curved path even when both wheels are exactly of the same diameter and are rotating at the same angular velocity. Although it is difficult to analytically calculate the magnitude of this disturbance, it can be easily determined experimentally. This disturbance, along with the one mentioned in item 1, can be compensated for by employing a correction factor in the controller algorithm. The correction factor multiplies the number of pulses arriving from one wheel. In our case the vehicle path, when loaded symmetrically, was always slightly curved to the left. Therefore, the number of pulses sampled from the left wheel is multiplied by 0.992, an experimentally determined correction factor. This correction factor causes the controller to slightly increase the left wheel speed (here by about 0.8%). In our experiments, this measure was found to substantially increase the vehicle's absolute position accuracy.

Finally, it is worthwhile to note that the nursing robot employs a system of navigation beacons in order to periodically update the vehicle's absolute position. Because of the high accuracy of the vehicle, the absolute updating is necessary only at the beginning and at the end of a specific task, namely, when the vehicle is at rest awaiting a new task.

References

(1) Koren, Y., Robotics for Engineers, McGraw-Hill Book Co. New-York, 1985. pp. 8-10.

(2) Weisbin, C., Saussure G., and Kammer, D.: "Self-Controlled, a Real-Time Expert System for Autonomous Mobile Robot," Computers in Mechanical Eng.. Sept. 1986, pp.12-19.

(3) Dorf R. C., Robotics and Automated Manufacturing, Prentice-Hall Co., Reston, 1983.

(4) Bauzil, G., Briot, M., and Ribes, P., "A Navigation Sub-System Using Ultrasonic Sensors for the Mobile Robot HILARE," 1st Int. Conf. on Robot Vision and Sensory Controls, Stratford-upon-Avon, UK., April 1981, pp. 47-58.

(5) Julliere, M., Marce, L., and Place, H., "A Guidance System for a Mobile Robot," Proc. of the 13th Int. Symp. on Industrial Robots and Robots, Chicago, Ill., April, 1983, pp. 13.58-13.68.

(6) Cooke, R.A., "Microcomputer Control of Free Ranging Robots," Proc. of the 13th Int. Symp. on Industrial Robots and Robots, Chicago, Ill., April 1983, pp. 13.109-13.120.

(7) Iijima, J., Yuta, S., and Kanayama, Y., "Elementary Functions of a Self-Contained Robot 'YAMABICO 3.1'," Proc. of the 11th Int. Symp. on Industrial Robots, Tokyo 1983, pp. 211-218.

(8) Fujiwara, K. and al., "Development of Guideless Robot Vehicle," Proc. of the 11th Int. Symp. on Industrial Robots, Tokyo 1983, pp 203-210.

(9) Nakamura, T., "Edge Distribution Understanding For Locating a Mobile Robot," Proc. of the 11th Int. Symp. on Industrial Robots, Tokyo 1981, pp. 195-202.

(10) Hollis, R., "NEWT, A Mobile, Cognitive Robot," BYTE, June 1977, pp. 30-45.

(11) Carlisle, B., "An Omni-Directional Mobile Robot," Developments in Robotics 1983, IFS Publications, Kempston, England 1983.

(12) Borenstein, J. and Koren, Y., "A Mobile Platform For Nursing Robots," IEEE Transactions on Industrial Electronics, June 1985.

(13) Moravec, H. P., "The CMU Rover," Proceedings of the National Conference of Artificial Intelligence, AAAI-82, August 1982, pp. 377-380.

(14) Moravec, H. P., "The Stanford Cart and the CMU Rover," Proceedings of the IEEE, Vol. 71, No 7, July 1983. pp. 872-884.

(15) Moravec, H. P., "Robots That Rove," Internal Report of the Robotics Institute, Carnegie-Mellon University.

(16) Moravec, H. P., "Three Degrees for a Mobile Robot," Internal Report of the Robotics Institute, Carnegie-Mellon University, July 1984.

(17) Tsumura, T., Fujiwara, N., Shirakawa, T., and Hashimoto, M., "An Experimental System for Automatic Guidance of Roboted Vehicle Following the Route Stored in Memory," Proc. of the 11th Int. Symp. on Industrial Robots, Tokyo 1981, pp. 187-193.

(18) Koren, Y., Computer Control of Manufacturing Systems, McGraw-Hill Book Co., New York 1983.

(19) Koren, Y., "Control of Machine Tools and Robots," Applied Mechanics Reviews, Vol. 39, No. 9, Sept. 1986, pp. 1331-1338.

(20) Fujii, S. et al., "Computer Control of a Locomotive Robot with Visual Feedback," Proc. of the 11th Int. Symp. on Industrial Robots, Tokyo 1981, pp. 219-226.

(21) Koren, Y., "Cross-Coupled Biaxial Computer Control for Manufacturing Systems," Transactions of the ASME, Journal of Dynamic Systems, Measurement and Control, Vol. 102, December 1980, pp. 265-272.

(22) Kuo, B. C., Analysis and Synthesis of Sampled-Data Control Systems, Prentice-Hall, Inc., Englewood Cliffs, N. J., 1983.

(23) Alberson, P., "Verifying Robot Performance," Robotics Today, Oct. 1983, pp. 33-36.